

# Phase shifters 응용을 위한 Sol-gel 법으로 제작된 (Pb<sub>0.5</sub>,Sr<sub>0.5</sub>)TiO<sub>3</sub> 박막의 열처리 온도에 따른 구조 및 유전 특성

황진호\*, 김경태\*, 김창일\*  
중앙대학교\*

## Dielectric and Structural of PST Thin Films with annealing temperature prepared by Sol-gel method for Phase shifters

Jin-Ho Hwang , Kyoung-Tae Kim\*, and Chang-Il Kim\*  
Incheon Polytech college, Chungang Uni.\*\*

### Abstract

(Pb,Sr)/TiO<sub>3</sub> (PST) thin films were fabricated by using the alkoxide-based sol-gel method. The PST stock solution was made and then spin-coated onto a Pt/Ti/SiO<sub>2</sub>/Si substrate. The coating and drying procedures were repeated several times, and the PST thin films were sintered at 450-650 C for 1 h. All PST thin films showed dense and homogeneous structures without the presence of any rosette structure. The thicknesses of the PST thin films were approximately 200 nm. The dielectric constant and the dielectric loss of the PST thin films sintered at 550 C were about 404 and 0.0023, respectively. The leakage current density of the PST thin film sintered at 550 C was 3.13 x 10<sup>-8</sup> A/cm<sup>2</sup> at 1 V.

**Key Words** : Dielectric properties; Sol-gel, Tunable,

### 1. 서론

Due to their unique properties, ferroelectric thin films are very attractive for applications to capacitors of dynamic random access memories (DRAMs), piezo micro-actuators, pyroelectric infrared detectors, and non-linear optical devices [1-5]. Among the various ferroelectrics, Pb(Zr,Ti)O<sub>3</sub> thin films have been intensively investigated while PbTiO<sub>3</sub> thin films have received less attention due to their high coercive field and large tetragonal distortion  $c/a$  of 1.064 [6, 7]. The addition of La or Sr decreases the coercive field and tetragonality [8]. It is well known, however, that the ferroelectric properties of PbTiO<sub>3</sub> deteriorate with decreasing film

thickness compared to those of the bulk ceramics. When the film thickness of PbTiO<sub>3</sub> is less than 1  $\mu$ m, the dielectric constant and the remanent polarization decrease [9].

A perovskite solid solution of PbTiO<sub>3</sub> and SrTiO<sub>3</sub> (PST) has the merits of the high dielectric constant of PbTiO<sub>3</sub> and the structural stability of SrTiO<sub>3</sub>. The properties of the Pb<sub>1-x</sub>Sr<sub>x</sub>TiO<sub>3</sub> bulk for  $x$  less than 0.7 are known to be ferroelectric with a tetragonal structure at room temperature [10]. To date, there have been a number of published papers dealing with the preparation and the dielectric properties of (Pb,Sr)TiO<sub>3</sub> bulk ceramics. However, there have been very few papers that deal with the dielectric properties of PST thin films for

DRAM applications.

Various deposition techniques, such as chemical vapor deposition (CVD), sputtering, laser ablation, and sol-gel, can be used for successful synthesis of the PST (or PT) system films. The sol-gel technique is especially useful for reducing processing costs, stoichiometric composition control, and large-area fabrication.

In this work,  $(\text{Pb}_{1-x}\text{Sr}_x)\text{TiO}_3$  thin film with  $x = 0.5$  were fabricated by using the sol-gel method, in which a PST metal alkoxide solution was used to spin coat them on Pt/Ti/SiO<sub>2</sub>/Si substrates. Their structural and dielectric properties were also investigated for DRAM applications.

## 2. 실험

$(\text{Pb}_{0.5}\text{Sr}_{0.5})\text{TiO}_3$  precursor solutions with excess Pb-acetate, 10wt %, were prepared by using the sol-gel method with Pb-acetate trihydrate  $[\text{Pb}(\text{CH}_3\text{CO}_2)_2 \cdot 3\text{H}_2\text{O}]$ , Sr-acetate  $[\text{Sr}(\text{CH}_3\text{CO}_2)_2]$ , and Ti iso-propoxide  $[\text{Ti}[\text{OCH}(\text{CH}_3)_2]_4]$  as starting materials, and 2-methoxyethanol ( $\text{CH}_3\text{OCH}_2\text{CH}_2\text{OH}$ ) as a solvent. The PST precursor solutions were spin-coated on the Pt/Ti/SiO<sub>2</sub>/Si substrates by using a spinner operated at 3000 rpm for 30 s and were then dried at 350 C for 10 min to remove the organic materials. This procedure was repeated several times then the films were sintered at temperatures from 450 to 650 C for 1 h to crystallize them into a perovskite structure. The final film thicknesses were about 200 nm, which was measured by scanning electron microscopy (SEM).

The powder precursors were examined by thermogravimetric analysis (TGA) / differential scanning calorimetry (DSC). The crystalline structures of the PST thin films were analyzed by using X-ray diffraction (XRD) with CuK emission. The surface and the cross-sectional microstructures were examined using SEM and the compositional depth profiles of the PST films interfacial layer and of the substrate were investigated by using Auger electron spectroscopy (AES). For electrical measurements, Pt films with a diameter of 300 nm were dc sputter-deposited as top electrodes. The dielectric constant and the dielectric loss were measured with an HP 4192A impedance analyzer. The leakage

current density was measured with an HP 4145B semiconductor parameter analyzer.

## 3. 결과 및 고찰

Measurements of the DSC and TGA curves of the dried PST powders were conducted, and the results are shown in Fig. 1. The weight loss of the dried powder derived from the sol-gel method was about 13.5 % at 800 C, as determined by the TGA curve. Endothermic peaks due to evaporation of the solvent and the absorbed water were observed at 100 C and 213 C, respectively. Due to combustion of the organic residues, exothermic peaks were observed in the temperature range from 290 C to 450 C. Due to the formation of the polycrystalline perovskite phase, exothermic peaks were observed around 500 C.

Figure 2 shows the XRD patterns of PST thin films prepared by using the sol-gel technique at sintering temperatures from 450 C to 650 C. All PST thin films showed the typical XRD pattern of a perovskite polycrystalline structure with no preferred orientation no pyrochlore phase was observed. Each film exhibited similar XRD patterns, so the difference in deposition temperature did not affect the crystallographic system.

Figure 3 shows the surface and the cross section of PST thin films sintered at 600 C. The PST film showed a dense and void-free grain structure with an average grain size of about 80 nm. As seen in the cross-sectional micrograph, the film consisted of submicron-sized fine grains with relatively flat surfaces, and the thicknesses of the films were approximately 200 nm.

Figure 4 shows the AES depth profile for the PST thin film sintered at 600 C. Diffusions of Pb, Sr, and Ti into the Pt bottom electrode were observed. From this result, we inferred that a nonstoichiometric perovskite PST layer was formed at the layer adjacent to the bottom electrode.

The dielectric constant and the dielectric loss of the PST thin films as a function of the frequency for various sintering temperatures are shown in Fig. 5. The dielectric constant increased with increasing sintering temperature the PST thin film

Figure 5 shows the dielectric constant of PST thin films sintered at 550 C as a function of the applied voltage. The capacitance was measured at 1 MHz with an amplitude of 0.1 V. The PST films showed their maximum dielectric constant at zero bias fields. The dielectric constant was found to decrease about 50% by increasing the applied bias up to 5 V. This may be due to space charge accumulation at the electrode interfaces. This charge accumulation was caused by the applied bias and Schottky potential of the metal electrodes [11]. The dielectric constant - applied voltage curve did not show any hysteresis, which indicated that the deposited films were paraelectric in nature.

Figure 6 shows the leakage current densities of the 200-nm-thick PST thin films as a function of the applied voltage for various sintering temperature. The leakage current density increased with increasing sintering temperature. This phenomenon can be probably explained by the facts that diffusion of Pb, Sr, and Tifrom the PST thin film into the Pt bottom electrode is more advanced at higher sintering temperature and a Pb-deficient interfacial layer was formed at the layer adjacent to the bottom electrode. The leakage current densities of the PST films sintered at 550 C and 600 C were less than 10<sup>-6</sup> A/cm<sup>2</sup> in the applied voltage range from 0 to 5 V.

#### 4. 결 론

In this research, PST thin films were prepared by using the sol-gel method to spin coat them on Pt/Ti/SiO<sub>2</sub>/Si substrates from PST metal alkoxide solutions. The thicknesses of the PST films were about 200 nm. All PST thin films showed dense and homogeneous structures without any presence of a rosette structure. The AES depth profile measurement showed, diffusion of Pb from the PST film into the Pt bottom electrode. The dielectric constant and the leakage current density increased with increasing sintering temperature, and the values for the PST thin film sintered at 600 C were 421 and 6.5 x 10<sup>-7</sup> A/cm<sup>2</sup>, respectively, at 3 V.

#### 참고 문헌

- [1] T. Kuroiwa, Y. Tsunemine, T. Horikawa, T. Makita, J. Tanimura, N. Mikami, and K. Sato, *Jpn. J. Appl. Phys.* **33**, 5187 (1994).
- [2] M. W. Cole, P. C. Joshi, M. H. Ervin, M. C. Wood, and R. L. Pfeffer, *Thin Solid Films* **374**, 34 (2000).
- [3] P. C. Joshi and M. W. Cole, *Appl. Phys. Lett.* **77**, 289 (2000).
- [4] D. Jung and K. N. Kim, *J. Korean Phys. Soc.* **39**, 80 (2001).
- [5] S. B. Kim, B. J. Min, D. P. Kim, and C. I. Kim, *J. Korean Phys. Soc.* **38**, 264 (2001).
- [6] B. Dibeneditto and C. J. Cronan, *J. Am. Ceram. Soc.* **51**, 364 (1968).
- [7] D. H. Chang, Y. S. Yoon, and S. J. Kang, *J. Korean Phys. Soc.* **38**, 277 (2001).
- [8] A. Li, C. Ge, D. Wu, P. L. S. Xiong, and N. Ming, *Mater.Lett.* **31**, 15 (1997).
- [9] B. Jiang and L. A. Bursill, *Phys. Rev. B* **60**, 9978 (1999).
- [10] B. Jaffe, W. R. Cook, Jr., and H. Jaffe, *Piezoelectric Ceramics*, (Academic Press, London, 1971), p. 119.
- [11] C. J. Brennan, *Proc. 3th. Int. Symp. Integrated Ferroelectrics*, Colorado Springs, p. 354 (1991).

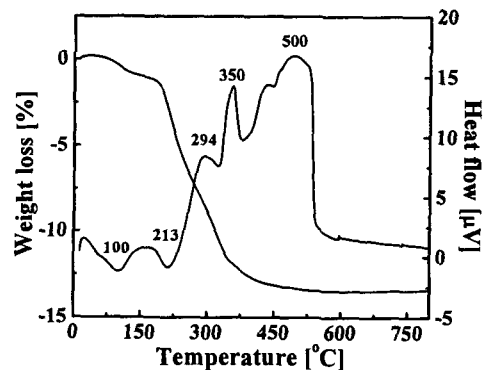


Fig. 1. DSC/TGA curves of the dried PST powders.

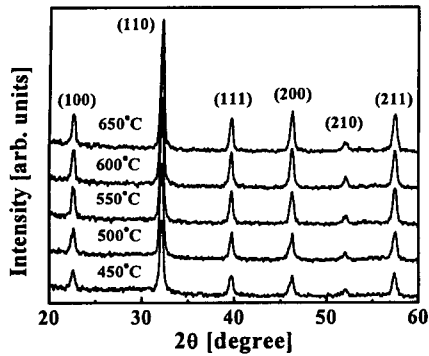


Fig. 2. X-ray diffraction patterns of PST thin films with various sintering temperature.

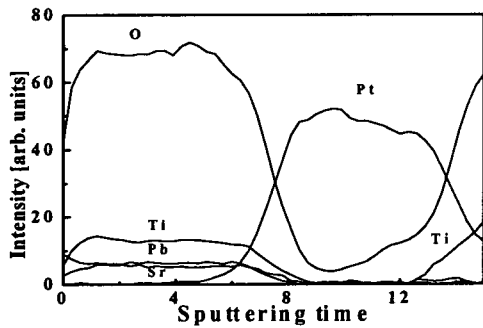


Fig. 3. AES analysis of PST thin film sintered at 600°C.

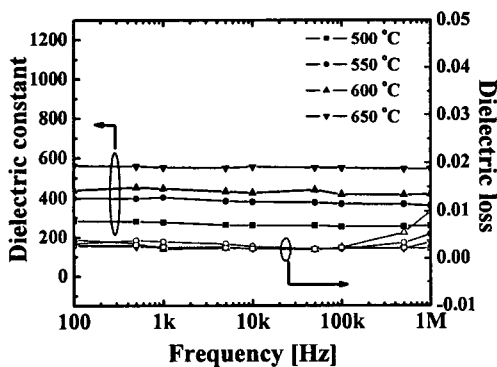


Fig. 4. Dielectric constant and dielectric loss as functions of the applied frequency for PST thin films with various sintering temperatures.

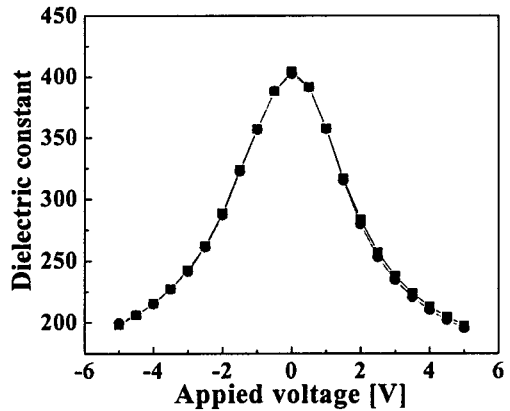


Fig. 5. Dielectric constant - applied voltage characteristics of PST thin films sintered at 550°C.

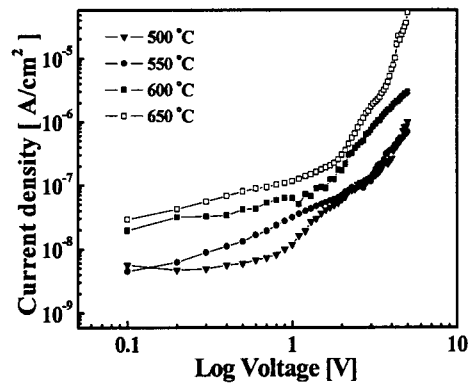


Fig. 6. Leakage current density of PST films as a function of the log (applied voltage) for various sintering temperature.